Study of intersubband transitions of $Zn_xCd_{1-x}Se/Zn_{x'}Cd_{y'}Mg_{1-x'-y'}Se$ multiple quantum wells grown by molecular beam epitaxy for midinfrared device applications

H. Lu,[a] A. Shen,[b] and M. C. Tamargo[c]
Department of Chemistry, The City College of the City University of New York, New York, New York 10031

W. Charles and I. Yokomizo
The Grove School of Engineering, The City College of New York, New York, New York 10031

M. Muñoz
Department of Physics, University of South Florida, Tampa, Florida 33620

Y. Gong and G. F. Neumark
Department of Applied Physics and Applied Mathematics, Columbia University, New York, New York 10027

K. J. Franz and C. Gmachl
Department of Electrical Engineering, Princeton University, Princeton, New Jersey 08544

C. Y. Song and H. C. Liu
Institute for Microstructural Sciences, National Research Council, Ottawa K1A 0R6, Canada

(Received 6 November 2006; accepted 12 March 2007; published 31 May 2007)

Two $Zn_xCd_{1-x}Se/Zn_{x'}Cd_{y'}Mg_{1-x'-y'}Se$ multiple quantum well structures were grown by molecular beam epitaxy. The quantum well layer thickness of the multiple quantum well region was varied in order to tune the intersubband transition energy. The high crystalline quality of the material was demonstrated by high resolution x-ray diffraction. Contactless electroreflectance (CER) spectroscopy and Fourier transform infrared (FTIR) spectroscopy were used to characterize the intersubband transitions. Excellent agreement between the estimated value obtained by CER and the value measured by FTIR was achieved. Intersubband absorption at 6.89 and 5.37 μm was observed demonstrating the ability to tune the properties of these wide band gap II-VI materials for mid-IR intersubband device applications. © *2007 American Vacuum Society.* [DOI: 10.1116/1.2723761]

I. INTRODUCTION

Devices that are based on intersubband (ISB) transitions, such as quantum cascade lasers and quantum well infrared photodetectors, are of great interest due to their potential advantages over devices based on interband transition in the infrared range.[1–3] Intersubband devices are usually made from multiple quantum well (MQW) structures and need a large band discontinuity to achieve operation at shorter wavelength and higher temperatures. MQW structures made of wide band gap II-VI materials $Zn_xCd_{1-x}Se/Zn_{x'}Cd_{y'}Mg_{1-x'-y'}Se$ are very promising candidates for short-wave midinfrared ISB device applications due to their large tunable band discontinuity.[4–6]

Modulation techniques, such as photoreflectance (PR) and contactless electroreflectance (CER), have been recognized as useful methods for understanding the physical properties of MQW and superlattice materials.[7–10] Contactless electroreflectance is a modulated technique[11,12] that measures the reflectivity changes produced by the presence of a periodic modulating electric field. This technique enables one to observe many band-to-band transitions besides the *E1-H1* transition. Therefore the ISB transition energies can be estimated. While PR and CER have previously been used to characterize many complex structures, including device structures such as heterojunction bipolar transistors (HBTs) and high electron mobility transistors[13] we only found one earlier report using PR (Ref. 9) to characterize ISB structures. Our study shows that by using CER we can accurately determine the ISB transition energy, and the result is confirmed by ISB absorption measured by Fourier transform infrared (FTIR) spectroscopy. The results also show the potential to tune the intersubband transition energy using these materials.

II. EXPERIMENT

A. Sample growth by molecular beam epitaxy (MBE)

In this work, two MQW samples were grown by MBE on semi-insulating InP (001) substrate using a dual-chamber Riber 2300P MBE system. This system has one chamber dedicated to III-V materials growth and another to the growth of II-VI compounds. The oxide desorption of the substrate was performed in the III-V growth chamber under an As flux. After the growth of a lattice-matched InGaAs buffer layer ($\sim$0.1 μm), the sample was transferred from the III-V chamber to the II-VI chamber and the InGaAs surface

[a]Current address: Materials Department, University of California, Santa Barbara, CA 93106-5050; electronic mail: luhong@engineering.ucsb.edu
[b]Also at Department of Electrical Engineering, CCNY, New York.
[c]Author to whom correspondence should be addressed; electronic mail: tamar@sci.ccny.cuny.edu

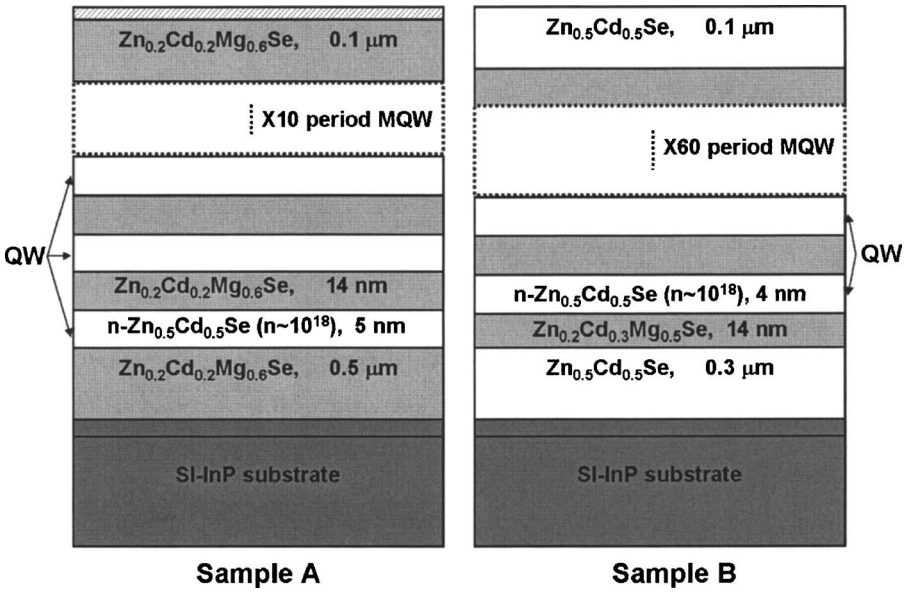

FIG. 1. Schematic layer structures of samples A and B. For both samples, the III-V buffer layer is InGaAs. Sample A is capped by CdSe to prevent the oxidation of the ZnCdMgSe layer.

was exposed to a Zn flux for 20 s, followed by the growth of a ZnCdSe buffer layer (~100 Å) grown at 170 °C. These steps for adjusting the III-V and II-VI interface are known to improve the material quality of the epitaxial layers.[14–16] The substrate temperature was then raised to 270 °C to grow the II-VI MQW structure. The VI/II beam equivalent pressure ratio was maintained between 3.5 and 4.0 during growth. This procedure has been previously used to produce epilayers with high crystalline quality and low defect density. The layer structures of these two MQW samples are shown in Fig. 1. Sample A has ten periods of $Zn_{0.5}Cd_{0.5}Se/Zn_{0.2}Cd_{0.2}Mg_{0.6}Se$ QWs sandwiched between two quaternary $Zn_{0.2}Cd_{0.2}Mg_{0.6}Se$ layers. Sample B has 60 periods of $Zn_{0.5}Cd_{0.5}Se/Zn_{0.2}Cd_{0.3}Mg_{0.5}Se$ QWs, in this case, sandwiched between two ternary $Zn_{0.5}Cd_{0.5}Se$ layers. The slight differences in the quaternary compositions were not intentional, but are due to the separation in time of the growth of the two structures. The nominal thicknesses of the wells are 50 and 40 Å in samples A and B, respectively, while the barriers are nominally 140 Å in both samples. In both samples, the QW layers are doped *n*-type using $ZnCl_2$ as dopant source to measure the ISB absorption. A doping level of $1-2\times10^{18}/cm^3$ for the QW layers and the growth rates (~0.6 μm/h for the ternary and 1.5 μm/h for the quaternary) were determined from calibration layers grown separately. To prevent the oxidation of Mg in the last layer of sample A, the structure was capped by a 90 Å thick CdSe layer.

B. Characterization techniques

The sample quality was established by high resolution x-ray diffraction (XRD) and photoluminescence (PL) measurements. The interband transitions in the samples were determined using CER.[11] The *E1-E2* intersubband transition was estimated and confirmed by FTIR measurement at RT.

XRD measurements showed that for both samples the ZnCdMgSe barrier and the ZnCdSe QW layers were nearly lattice matched to the InP substrate. Figure 2 is the high resolution XRD curve of sample A. The thickness of one period (one barrier and one QW) of 197 Å was calculated from the satellite peaks and agrees well with the designed value. Due to the slightly different composition, the band gaps of the quaternaries in samples A and B are 3.1 and 3.0 eV, respectively, obtained by the 77 K PL measurements. The PL measurements were performed using the 325 nm line of a He–Cd laser as an excitation source. Intense and narrow PL emission peaks from the QWs in sample A were observed at 549 nm (2.26 eV, 77 K) and 569 nm [2.18 eV, RT, shown by the dashed-dot line in Fig. 3(a)], with no trace of any deep level emissions. Due to the strong absorption of the thick ZnCdSe cap layer, the PL emission from the QWs in sample B is weak and could only be measured at 77 K [2.275 eV, shown in Fig. 3(b)].

The CER measurements were taken at room temperature using the light from a 150 W xenon-arc lamp. The light intensity at wavelength λ, $I_0(\lambda)$, is focused onto the sample by means of a lens. The reflected light is collected by a second

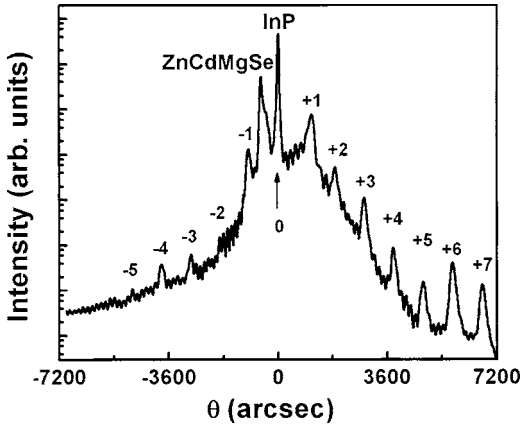

FIG. 2. High resolution x-ray diffraction curve of sample A.

lens and is focused onto a Si photodetector. The sample was placed in a condenserlike system consisting of a front wire grid electrode with a second metal electrode separated from the first electrode by insulating spacers. The dimensions of the spacer are such that there is a very thin layer (~0.1 mm) of air (or vacuum) between the front surface of the sample and the wire grid of the first electrode. Thus, there is nothing in direct contact with the front surface of the sample. The electromodulation was achieved by applying an ac voltage of 1 kV (peak to peak), 200 Hz across the electrodes.

The light striking the detector contains both dc and ac signals: the dc signals given by $I_0(\lambda)R(\lambda)$, where $R(\lambda)$ is the dc reflectance of the material while the modulated (ac) signal (at frequency Ω_m) is $I_0(\lambda)\Delta R(\lambda)$, where $\Delta R(\lambda)$ is the change in reflectance produced by the modulation source. The ac signal from the detector, proportional to $I_0(\lambda)\Delta R(\lambda)$, is measured by a lock-in amplifier. Typically $I_0\Delta R$ is 10^{-4} to 10^{-6} of I_0R. In order to evaluate the quantity of interest, i.e., the relative change in reflectance $\Delta R/R$, a normalization procedure must be used to eliminate the uninteresting common feature $I_0(\lambda)$. The normalization is performed by a variable neutral density filter (VNDF) connected to a servo mechanism. The dc signal from the detector, which is proportional to $I_0(\lambda)R(\lambda)$, is fed into the servo which moves the VNDF in such a manner as to maintain a constant $I_0(\lambda)R(\lambda)$, i.e., $I_0(\lambda)R(\lambda)=C$. Under these conditions the ac signal $I_0(\lambda)\Delta R(\lambda)=C\Delta R(\lambda)/R(\lambda)$. Subsequently, the signal to the lock-in amplifier is proportional to the quantity of interest, i.e., $\Delta R(\lambda)/R(\lambda)$.

The intersubband absorption was measured using FTIR spectrometer equipped with a liquid-nitrogen (LN_2) cooled HgCdTe detector. The sample was polished to obtain a multiple-pass geometry (see inset of Fig. 4).

III. RESULTS AND DISCUSSION

The CER spectra of the two MQW samples are shown in Figs. 3(a) and 3(b). In both, the solid line is the CER spectrum measured at room temperature. The transition energies were obtained using a fit (shown by the dashed line) based on the first derivative of a Gaussian line shape, which is the appropriate line shape due to the bound origin of the transitions.[7,8] The arrows in Fig. 3 indicate all the energy values of the transitions resulting from the fit. These values are also presented in Table I. The notation $EnH(L)m$ represents the transition from the nth conduction subband to the mth valence subband of heavy (H) or light (L) hole character, respectively. Comparing the two CER spectra, the signal from sample B contains more noise than that of sample A. This may be due to roughening of the surface after etching. [A 70 s chemical etching was performed on sample B using 0.1M bromine-methanol solution since the signal (at ~2.1 eV) from the thick ZnCdSe top layer would dominate the CER spectrum.] Furthermore, to avoid the effect of oxidation on the etched surface, only two CER scans were done for sample B, while 20 scans were used for the measurement on sample A, improving the signal to noise ratio in sample A.

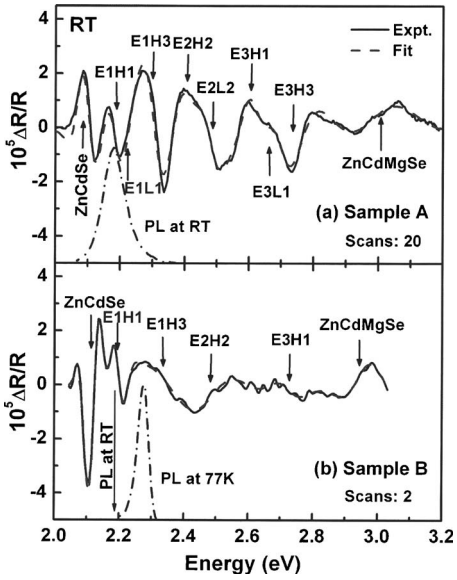

FIG. 3. CER spectra at room temperature (RT) of (a) sample A and (b) sample B. The solid line represents the experimental data. The dashed line is a fit based on the first derivative of a Gaussian line shape, yielding the transition energies indicated by the arrows. The room temperature PL emission of sample A and the 77 K PL emission of sample B, used to identify the *E1H1* transition, are shown in 3(a) and 3(b), respectively.

Due to the relatively high noise level of CER spectrum of sample B, we did not try to fit the *EnLm* transitions.

The assignments were done according to the following considerations. First, the signals at 3.00 and 2.96 eV were assigned to the ZnCdMgSe barriers by comparison to the 77 K PL emissions from the barriers, which were observed at 3.1 and 3.0 eV, respectively, and considering the thermal energy shift from 77 K to room temperature. The signals at ~2.1 eV in Figs. 3(a) and 3(b) were assigned to the transition of ZnCdSe grown lattice matched to the InP substrate according to previous reports.[17] The CER transitions at 2.183 and 2.196 eV were assigned to the *E1H1* transitions for samples A and B, by comparing with the PL emission signals, included in Figs. 3(a) and 3(b) and Table I. The QW PL signal for sample B was only measured at 77 K, as indicated in the experimental section, and a shift of ~80 meV due to the temperature.

In order to assign the remaining transitions calculations were performed based on the envelope function approximation, considering that the QW was doped.[18,19] The values for the effective masses and spin-orbit splitting used in this calculation were obtained from a linear interpolation of the binaries values.[4] Following the reported values for the conduction band offset (CBO) in Refs. 4 and 5, we have assumed that the CBO is 80% of the band gap difference between the barriers and wells. A QW thickness of 52 Å for sample A and 42 Å were obtained from these calculations. The identified transitions correspond to the symmetry allowed ($n=m$) and symmetry forbidden but parity allowed ($n=m\pm2,4\ldots$) transitions. As seen in Table I, the calculations agree well with the measured values. The *E1-E2* ISB transition energies of the two samples can be estimated to be 178 and 233 meV,

TABLE I. Experimental and calculated transition energies of the MQW structures.

	Sample A (d_{QW}=52 Å)		Sample B (d_{QW}=42 Å)	
IB transition	Calculation (eV)	CER (eV) (±0.005)	Calculation (eV)	CER (eV) (±0.005)
ZnCdSe	2.105 (RT PL)	2.098	2.183 (77 K PL)	2.120
E1H1	2.181	2.183	2.191	2.196
E1L1	2.205	2.205		
E1H3	2.300	2.306	2.333	2.336
E2H2	2.405	2.412	2.487	2.490
E2L2	2.496	2.483		
E3H1	2.606	2.608	2.712	2.724
E3L1	2.630	2.633		
E3H3	2.725	2.726		
Barrier	3.10 (77 K PL)	3.000	3.00 (77 K PL)	2.958
ISB transition	Estimation (meV)	FTIR (meV)	Estimation (meV)	FTIR (meV)
E1-E2	178	180	233	231

which correspond to wavelengths of 6.97 and 5.32 μm.

The predicted values of the *E1-E2* transitions were confirmed by FTIR measurements. The absorbance for each sample is obtained by taking the negative logarithm of *P*-polarized transmittance over *S*-polarized transmittance. The normalized absorbances of the two samples are shown in Fig. 4. Absorption peaks at 180 meV (6.89) and 231 meV (5.37 μm) are clearly observed and they are strongly polarization dependent. The full width at half-maxima are 21 and 30 meV, indicating a ratio of $\Delta E/E_{peak}$ of 10% for both samples. This suggests that the absorption is due to the bound-to-bound ISB transition *E1-E2*. Comparison between the FTIR results and the CER predictions indicates that an excellent agreement was achieved. This work also demonstrates the ability to readily tune the absorption wavelength of the ISB transitions in our materials by changing the QW thickness.

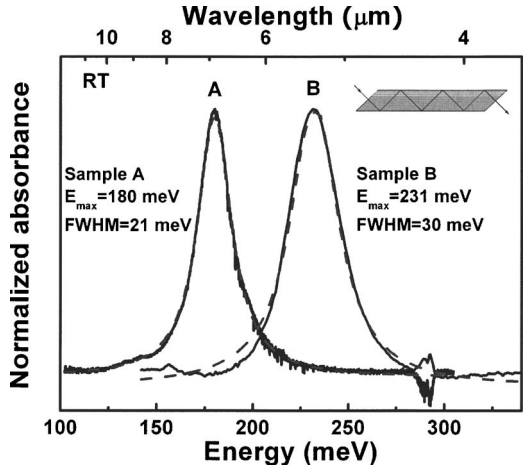

FIG. 4. Intersubband absorption (solid line) measured by FTIR at RT and Lorentzian fit (dashed line) for samples A and B. The inset indicates the multiple-pass geometry used in the measurements.

IV. CONCLUSION

We have grown two $Zn_xCd_{1-x}Se/Zn_{x'}Cd_{y'}Mg_{1-x'-y'}Se$ MQW structures having different QW thickness, which allows us to tune the ISB transition energy in the mid-IR region. Excellent material quality, consistent with the requirements of device applications, has been demonstrated. Using CER and envelope function approximation calculations, the ground state and higher order transitions were observed and identified. From this, the *E1-E2* ISB transition energies of these two structures were estimated as 178 and 233 meV. Intersubband absorption measurements by FTIR yielded peak values at 180 and 231 meV. The excellent agreement between these two techniques shows that CER can be used to investigate structural, optical, and electronic properties of these complex structures, including prediction of the ISB transition energy. These results give further confirmation that MQW of this II-VI material system can be grown in high quality and can be designed to fabricate ISB devices whose operating wavelengths can be readily tuned in the mid-IR range by changing the QW thickness.[20]

ACKNOWLEDGMENTS

This work was supported by NASA Grant No. NCC-1-03009, NSF Grant No. EEC-0540832 through MIRTHE-ERC, and the Center for Analysis of Structures and Interfaces (CASI). Special thanks to Dr. S. K. Zhang and Dr. R. R. Alfano, and Dr. D. Crouse for helpful discussions and support. One of the authors (K.J.F.) acknowledges the support of the NSF Graduate Research Fellowship Program.

[1] *Intersubband Transitions in Quantum Wells: Physics and Device Applications I & II, Semiconductors and Semimetals*, edited by H. C. Liu and F. Capasso (Academic, San Diego, 2000), Vols. 62 and 66.
[2] B. F. Levine, J. Appl. Phys. **74**, R1 (1993).
[3] C. Gmachl, F. Capasso, D. L. Sivco, and A. Y. Cho, Rep. Prog. Phys. **64**, 1533 (2001).
[4] M. Muñoz, H. Lu, X. Zhou, M. C. Tamargo, and F. H. Pollak, Appl. Phys. Lett. **83**, 1995 (2003).

[5]M. Sohel, X. Zhou, H. Lu, M. N. Perez-Paz, M. Tamargo, and M. Muñoz, J. Vac. Sci. Technol. B **23**, 1209 (2005).
[6]H. Lu, A. Shen, S. Y. Song, H. C. Liu, S. K. Zhang, R. R. Alfano, M. C. Tamargo, and M. Muñoz, Appl. Phys. Lett. **89**, 131903 (2006).
[7]F. H. Pollak and H. Shen, Mater. Sci. Eng., R. **10**, 275 (1993).
[8]O. J. Glembocki and B. V. Shanabrook, in *Semiconductors and Semimetals*, edited by R. K. Willardson and A. C. Beer (Academic, New York, 1992), Vol. 36, p. 221.
[9]P. A. Dafesh, J. Appl. Phys. **71**, 5154 (1992).
[10]G. Sęk, J. Misiewicz, K. Regínski, and J. Muszalski, Vacuum **48**, 283 (1997).
[11]F. H. Pollak, *Group III Nitride Semiconductor Compounds* (Clarendon, Oxford, 1998).
[12]M. Cardona, *Modulation Spectroscopy* (Academic, New York, 1969).
[13]Y. S. Huang and F. H. Pollak, Phys. Status Solidi A **202**, 1193 (2005).
[14]S. P. Guo and M. C. Tamargo, *II-VI Semiconductor Materials and Their Applications* (Taylor and Francis, New York, 2002), Vol. 12.
[15]L. Zeng, B. X. Yang, M. C. Tamargo, E. Snoeks, and L. Zhao, Appl. Phys. Lett. **72**, 1317 (1998).
[16]L. Zeng, S. P. Guo, Y. Y. Luo, W. Lin, M. C. Tamargo, H. Xing, and G. S. Cargill III, J. Vac. Sci. Technol. B **17**, 1255 (1999).
[17]T. Holden, P. Ram, F. H. Pollak, J. L. Freeouf, B. X. Yang, and M. C. Tamargo, Phys. Rev. B **56**, 4037 (1997).
[18]G. Bastard and J. A. Brum, IEEE J. Quantum Electron. **QE-22**, 1625 (1986).
[19]G. Bastard, *Wave Mechanics Applied to Semiconductor Heterostructures* (Les Editions de Physique, Paris, France, 1988).
[20]H. Lu, A. Shen, M. Muñoz, M. N. Perez-Paz, M. Sohel, S. K. Zhang, R. R. Alfano, and M. C. Tamargo, Phys. Status Solidi B **243**, 868 (2006).